

4.4. COMPUTED TOMOGRAPHY OF THE VERTEBRAL COLUMN AND COELOMIC STRUCTURES IN THE NORMAL LOGGERHEAD SEA TURTLE (*CARETTA CARETTA*)



Valente, A.L.; Cuenca, R.; Zamora, M.A.; Parga, M.L.; Lavín, S.; Alegre, F. y Marco, I. (2006). Computed tomography of the vertebral column and coelomic structures in the normal loggerhead sea turtle (*Caretta caretta*). Vet. J. (2006), doi: 10.1016/j.tvjl.2006.08.018.



Computed tomography of the vertebral column and coelomic structures in the normal loggerhead sea turtle (*Caretta caretta*)

A.L.S. Valente^{a,*}, R. Cuenca^a, M. Zamora^b, M.L. Parga^c,
S. Lavin^a, F. Alegre^c, I. Marco^a

^a *Servei d'Ecopatologia de Fauna Salvatge, Facultat de Veterinària, Universitat Autònoma de Barcelona, 08193 Bellaterra, Barcelona, Spain*

^b *Diagnòstic Mèdica, Còrcega, 345 Barcelona, Spain*

^c *Centre de Recuperació d'Animals Marins, Camí Roal, 239 08330 Premià de Mar, Barcelona, Spain*

Accepted 31 August 2006

Abstract

The aim of this study was to determine the normal computed tomography (CT) appearance of the vertebral column and coelomic structures of the loggerhead sea turtle (*Caretta caretta*) and to use three-dimensional (3D) and multiplanar reconstructions to indicate the position of each organ in relation to the vertebrae and carapace. Transverse sections of 1 mm thickness were performed in seven clinically healthy and in five dead loggerhead sea turtles using multi-detector CT equipment. A computer workstation was used for multiplanar and 3D reconstructions. Dead turtles were frozen and sectioned in the transverse, dorsal and sagittal planes to compare the anatomical structures' appearance with CT images. Clinically relevant organs including the oesophagus, stomach, trachea, bronchi, lungs, liver, gallbladder, heart, spleen, kidneys and vertebral canal were identified in CT images. Computed tomography provides detailed information on the respiratory system and skeleton; the location of the coelomic structures with respect to the carapace and the vertebrae that is provided in this work will facilitate the use of other ancillary diagnostic techniques such as ultrasound, radiography and biopsy, thereby improving safety of access in surgical procedures.

© 2006 Elsevier Ltd. All rights reserved.

Keywords: Computed tomography; Diagnostic imaging; Cross-sectional anatomy; Chelonians; Three-dimensional reconstruction

1. Introduction

At marine animal rehabilitation centres, sea turtles are often admitted with traumatic and pulmonary disorders (Pont and Alegre, 2000; Orós et al., 2005). Most traumatic problems affect the flippers or the carapace and are mainly due to entrapment in fishing nets and collision with boat propellers. Due to the dorsal position of the lungs, which are in close contact with the carapace, pulmonary disease often occurs secondary to traumatic injuries of the carapace (Orós et al., 2005).

In sea turtles the axial skeleton is composed of the carapace, plastron bones, vertebrae, ribs and derivatives of the

ribs (Wyneken, 2001). The carapace is formed by the scutes which form the outermost layer of the shell and by the bony plates which are the main structural components of the shell. The multiple scutes overlap the bony plates (neural, pleural and peripheral bones) which are fused with the vertebrae or ribs forming a single carapace bone. Neural bones are those that cover the vertebral column. Pleural bones are formed by the ribs and their dermal (ossified) extensions, and the peripheral bones form the margin of the carapace. In most lung disorders and shell or skeletal injuries in the turtle, plain radiographic data do not reveal the extent of complex fractures due to superimposed bone structures (Abou-Madi et al., 2004).

Compared with conventional radiography, computed tomography (CT) allows better distinction of specific tissue densities and discrete changes in organ size, shape, margin

* Corresponding author. Tel.: +34 93 581 19 23; fax: +34 93 581 20 06.
E-mail address: schifinoval@hotmail.com (A.L.S. Valente).

contour and position (Gaudron et al., 2001). Computed tomography is a non-invasive, cross-sectional diagnostic imaging technique that offers significant advantages for detection of pathologies in chelonians, and is ideal for diagnosing skeletal and soft tissue abnormalities (Gumpenberger and Henninger, 2001).

Multi-detector Computed Tomography (MDCT) technology has rapidly and drastically changed the way CT has been used in recent years. By using multiple rows of detector arrays instead of a single detector, MDCT can produce highly accurate three-dimensional (3D) volume data sets allowing reconstruction of the total body, tracheo-bronchial and pulmonary volume rendering, virtual bronchoscopy and colonoscopy, and volumetric reconstruction of the skeleton. In addition, MDCT provides faster and more detailed scanning results, an important consideration in wild animals (ASIH/HL/SSAR, 2001) as it minimizes the deleterious effects of prolonged sedation or physical restraint. Although due to its cost it is not used routinely in veterinary medicine, it is important to recognize that the amount of information it provides in a short-time period may justify its use in endangered species.

Although some publications on CT in other chelonians exist (Gumpenberger and Henninger, 2001; Raiti and Haramati, 1997; Raiti, 1998; Wilkinson et al., 2004; Wyneken et al., 2000), to the authors' knowledge there is only one CT study on the head of the loggerhead sea turtle (*Arenicbia* et al., 2005). No published data concerning the use of CT in the coelomic cavity of this species were found.

Accurate interpretation of multiplanar and 3D CT images of the loggerhead sea turtle requires comparative cross-sectional anatomy images of this species. The purpose of this study was to provide normal CT images of the vertebral column and coelomic structures of the loggerhead sea turtle (*Caretta caretta*), thereby establishing reference standards for organ size and position in this species, and to provide images of virtual tracheo-bronchoscopy and 3D reconstructions of the respiratory tract and bone structures. In the present study we used a combination of CT imaging and gross anatomical sections that allowed accurate identification of the anatomical structures.

2. Materials and methods

Computed tomography was performed in 12 loggerhead sea turtles (seven live: juvenile; and five dead: four juvenile and one subadult). All turtles were accidentally caught in pelagic long line sets and fishing nets off the north-western Mediterranean coast (40°31'–42°26'N and 0°32'–3°10'E) of Spain, and were temporally housed in the rehabilitation facilities of the Rescue Centre for Marine Animals (CRAM), in Premià de Mar, Barcelona, Spain. Only clinically normal animals were included in this study. Dead turtles were kept frozen until the examination and were thawed 24–48 h before the CT procedure, depending on their size.

Live turtles were anaesthetized with a combination of ketamine (15 mg/kg, Imalgene 1000, Merial) and diazepam

(0.5 mg/kg, diazepam, Almirall Proderfarma), injected intravenously in the dorsal cervical sinus to avoid head and flipper movement. Cardiac frequency was verified using a mini-doppler (Doppler High Sensitivity Pocket Doppler D900, Huntleigh Healthcare Ltd.) and the animals were carefully kept wet prior to the scan. No intravenously or orally administered contrast material was used, and all animals were positioned in ventral recumbency for the examination.

Computed tomography of the vertebral column and coelomic structures were obtained by a 16-detector row CT scanner (Aquilion 16, Toshiba Medical) using the following parameters: 120 kVp, 250 mA, 16 × 1 mm detector configuration and a 512 × 512 matrix. The field of view ranged from 35 to 52 cm and total examination time was from 10 to 15 s, depending on the size of the turtle. The volumetric reconstruction of image sections with a 1 mm slice width and interval of 0.8 mm were performed. Although the original MDCT sections were taken using 1 mm thickness, better images were obtained after manipulation and adjusting to sections of 4 mm. Multiplanar reformatted images and 3D volume-rendered images were generated on a Vitrea computer workstation (Vitrea version 3.0.1., Vital Images). We used bone and parenchymal filters to improve contrast between the different structures.

In order to carry out the anatomical study and establish a comparison with the MDCT images, the previously scanned dead turtles were placed in individual right-angled polystyrene boxes and these were filled with tap water. The boxes with the cadavers were refrozen at –80 °C for at least 24 h before anatomical sectioning. The turtles were sectioned in a pre-determined plane: transverse, dorsal or sagittal. Serial parallel slices from 18 to 20 mm thickness were obtained using an electric bone saw. Slices were immediately washed with 80% ethanol to eliminate frost build-up and to remove debris, and separated by grids. After labelling, the frozen slices were embedded for 30 min in neutral-buffered 10% formalin solution for thawing. For recording of the fresh surface, a digital high-resolution, 2560 × 1920 pixels camera (Digital Still Camera, Sony DSC-F707, Sony Corporation) was used in daylight. Further transformations of the images such as rotation, scaling, cutting, filtering, and corrections to contrast, brightness and colour were performed with Adobe Photoshop (v 5.5). For each anatomical slice, a corresponding CT image was chosen, and identifiable anatomical structures were labelled on the cadaver sections and on the corresponding CT images. The terminology applied to the anatomical structures corresponded to that of the *Nomina Anatomica Veterinaria*; however, specific terminology for sea turtles (Wyneken, 2001) was also applied.

3. Results

With regard to skeletal structures, multiplanar sagittal reconstruction of the vertebral column permitted evaluation of the vertebrae and the vertebral canal, which was

wider in the cervical region than in the other regions of the vertebral column (Fig. 1). The lateral and ventral views of the 3D volume rendering of the vertebral column showed the morphology and arrangement of the vertebrae (Fig. 1). Eight cervical vertebrae were identified (Fig. 1). The ventral part of the atlas was clearly seen in the sagittal multiplanar reconstruction of the vertebral column (Fig. 1).

The intervertebral foramina were easily recognizable in the cervical region being greatest between the seventh and eighth vertebrae (Fig. 1). In the dorsal region, these foramina were not seen between the vertebral arches but rather, as a series of large foramina positioned dorsally and centrally relative to the vertebral bodies, between the vertebral arch and their respective neural bones (Fig. 1) being the exit of the spinal nerve roots from the vertebral canal (Fig. 2). From the ninth dorsal vertebra caudally, the intervertebral foramina reappeared between the vertebral arches (Fig. 2).

The intervertebral space was broad in the cervical region and decreased caudally, becoming almost unrecognizable between the 7th and 10th dorsal vertebrae. Between the 10th dorsal and first sacral vertebra the space was again visible (Figs. 1 and 2). The first dorsal vertebra and the

8–10th dorsal vertebra all had a short body (Fig. 1). The scapula was attached to the first pleural bone immediately cranial to the first pair of ribs, where a non-ossified area was seen in the carapace of a small juvenile turtle (Fig. 2). From the three sacral vertebrae, only the first two were attached to the ileum (Fig. 2). The bodies of the caudal vertebrae showed a thick cartilaginous plug on each end; these vertebrae varied in number, ranging from 13 to 17 vertebrae. The arches and processes also became progressively shorter (Fig. 2).

Clinically relevant organs and anatomical structures including the oesophagus, stomach, trachea, bronchi, lungs, liver, gallbladder, heart, spleen and kidneys were identified in the CT images with the aid of the anatomical sections. The normal appearance and position of the coelomic organs identified on the MDCT images and their relation to the carapace and the vertebral column are indicated in Figs. 3 and 4.

The ventral view of the whole body 3D reconstruction indicating the cranial and caudal border of the heart showed that this organ is located in an area not protected by the plastron bones (Fig. 3).

The liver lobes could be distinguished in the CT images in all sections, but the distinction between the hepatic parenchyma and pectoral musculature was not clear due to lack of contrast (Fig. 3). It was possible to identify the gallbladder in the transverse and dorsal sections (Fig. 3).

The trachea and oesophagus were easily recognizable. The trachea was observed ventral and to the right of the oesophagus and maintained this position from the level of the second to the fourth cervical vertebra (Fig. 5). The carina was seen at the level of the first dorsal vertebra (Fig. 5). When evaluated using virtual bronchoscopy, the tracheal mucosa was seen to have a smooth surface (Fig. 5). The extra and intrapulmonary parts of the bronchi were identified clearly in the 3D pulmonary rendering (Fig. 6). The external part of the left bronchus crossed ventrally to the oesophagus (Fig. 1).

The morphology of the lungs, bronchi and pulmonary blood vessels could be distinguished, and the central intrapulmonary bronchus was clearly seen in the transverse sections (Fig. 6). Each central bronchus extended dorsally and longitudinally into the lung, and had numerous airways extending from it (Fig. 7). The lungs were not lobed (Figs. 6 and 7), and the pulmonary parenchyma was strongly reticulated (Fig. 8). Large vessels such as the aorta and the vena cava could not be identified in the mediastinal space as they are usually seen in mammalian species. Two large pulmonary blood vessels around the central bronchus could be identified in all sections. They extended longitudinally parallel to the bronchus (Fig. 7). The pulmonary artery and vein were identified histologically dorsal and ventral to the central bronchus, respectively (Fig. 6).

Only the external silhouette of the kidneys was identifiable, immediately caudal to the lungs, in the transverse section (Fig. 9).

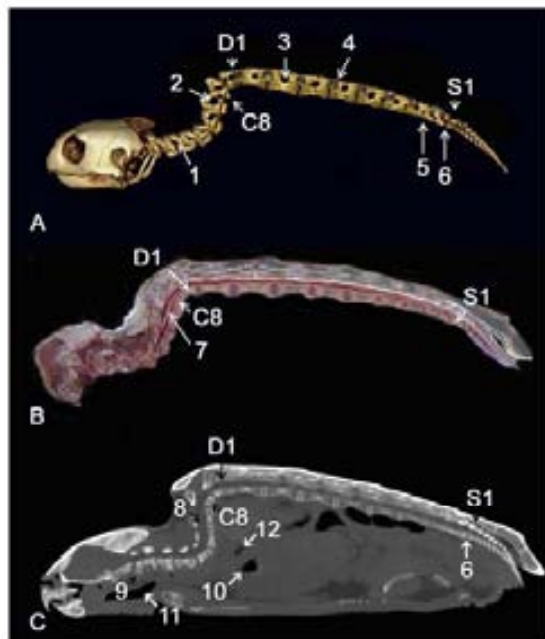


Fig. 1. (A) 3D CT reconstruction, (B) sagittal gross anatomical section and (C) CT multiplanar reconstruction (sagittal plane) of the vertebral column of a juvenile loggerhead sea turtle. A: 1 and 2, intervertebral foramina in the cervical vertebrae; 3, intervertebral foramina in the dorsal vertebrae; 4, costovertebral joint (costocentral joint); 5 and 6, intervertebral spaces. C8: 8th cervical vertebra; D1, 1st dorsal vertebra; S1, 1st sacral vertebra. B: 7, vertebral canal and spinal cord. C: 8, cervical vertebral canal; 9, ventral portion of the atlas; 10, transverse section of the left bronchus; 11, trachea; 12, oesophagus/lumen.

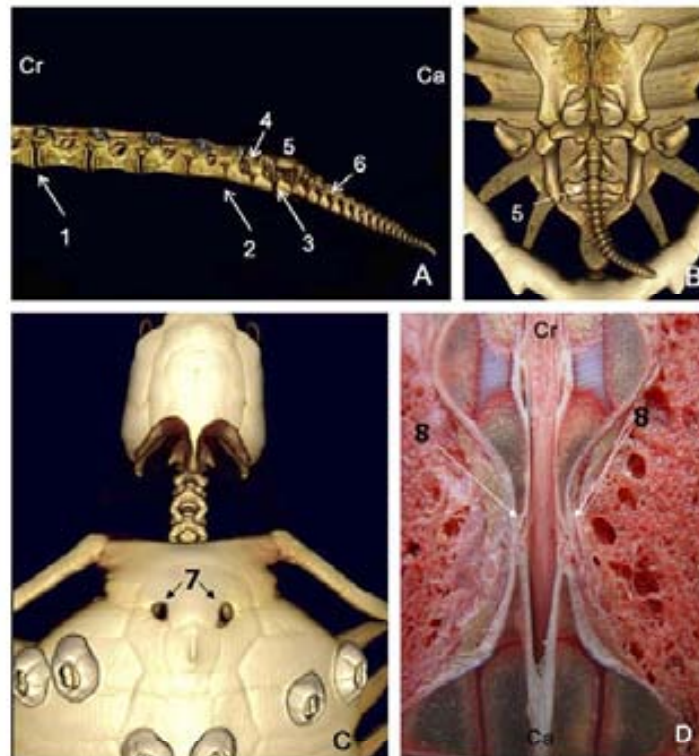


Fig. 2. (A) Lateral and (B) ventral views of 3D CT reconstructions of the vertebral column (sacral and caudal regions), (C) dorsal views of the 3D CT reconstructed carapace and (D) dorsal gross anatomical section of a juvenile loggerhead sea turtle. 1, intervertebral space between the 4th and 5th dorsal vertebrae; 2, intervertebral space between the 8th and 9th dorsal vertebrae; 3, intervertebral space between the 10th dorsal vertebra and 1st sacral vertebra; 4, intervertebral foramen placed between the vertebral arches; 5, 1st sacral vertebra; 6, caudal vertebrae; 7, non-ossified area in the carapace; 8, root of spinal nerves.

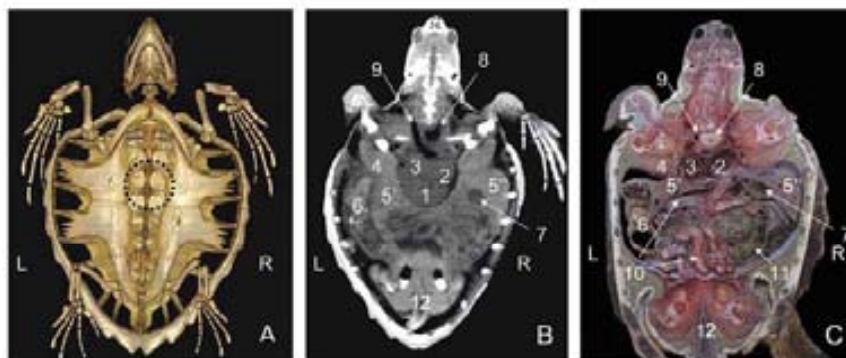


Fig. 3. (A) Ventral view of the skeleton 3D CT reconstruction, (B) multiplanar CT reconstruction (dorsal plane - soft-tissue window) and (C) dorsal gross anatomical section of a juvenile loggerhead sea turtle. A: Indicated area corresponds to the cardiac region. B and C: 1, ventricle; 2, right atrium; 3, left atrium; 4, pectoral musculature; 5 and 5', left and right hepatic lobes, respectively; 6, stomach; 7, gallbladder; 8, oesophagus; 9, trachea; 10, small intestine; 11, large intestine; 12, rectum.

4. Discussion

Computed tomography and 3D reconstruction have a role in the diagnosis of a wide range of diseases in a variety

of animals (Garland et al., 2002). In our study the 3D volume rendering of the skeleton allowed a clear view of the arrangement of the structures in their natural position. The turtles were sedated because the CT examination was

Please cite this article in press as: Valente, A.L.S. et al., Computed tomography of the vertebral column and coelomic ..., Vet. J. (2006), doi:10.1016/j.tvjl.2006.08.018

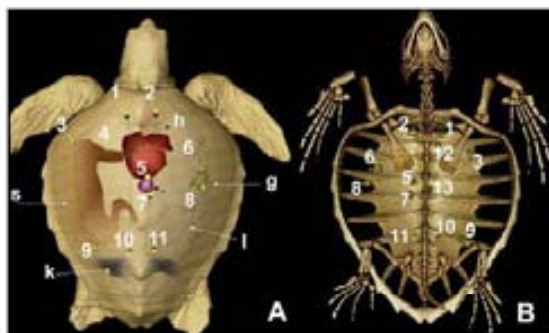


Fig. 4. (A) Dorsal and (B) ventral view of 3D CT reconstructions of the skeleton (plastron bones were removed in B) of a juvenile loggerhead sea turtle. Dots indicate the limits of each organ. 1, 2 cranial borders of the lungs; 3, cranial border of the stomach; 4, position of the cardia (seen only in A); 5, cranial border of the spleen; 6, cranial border of the gallbladder; 7, caudal border of the spleen; 8, caudal border of the gallbladder; 9, caudal border of the stomach; 10–11, caudal border of the lungs; 12, 13 cranial and caudal border of the heart, respectively (seen only in B). Stomach (s), lungs (l), heart (h), spleen (sp), gallbladder (g) and kidneys (k) were illustrated in A.

preceded by another diagnostic imaging procedure. However, considering the short time (10–15 s) required for a turtle examination we believe that this procedure could be carried out without chemical restraint.

The presence of an “intervertebral foramen” located dorsal to each vertebral body, from the 1st to the 8th dorsal vertebra instead of between the neural arches of adjacent vertebra seems a peculiarity of chelonians, since in this group of reptiles the neural arches are directly fused and the nerve roots do not exit via the intercentral joints (between the vertebral bodies) as they do in mammals. Differences in width of the intervertebral space seemed to be related to the shape of the vertebral centra and how they are joined to each other. The shapes of articulating surfaces at the ends of the vertebral centra of reptiles are of evolutionary and functional importance (Gaffney, 1990). We have found cervical vertebra of the loggerhead sea turtle to be predominately *procoelus* (the front of the *centrum* is concave and the rear of the *centrum* is convex) whereas the dorsal ones seemed to be weakly *amphicoelus*. In *amphicoelus* vertebrae the cranial and caudal ends of the cen-

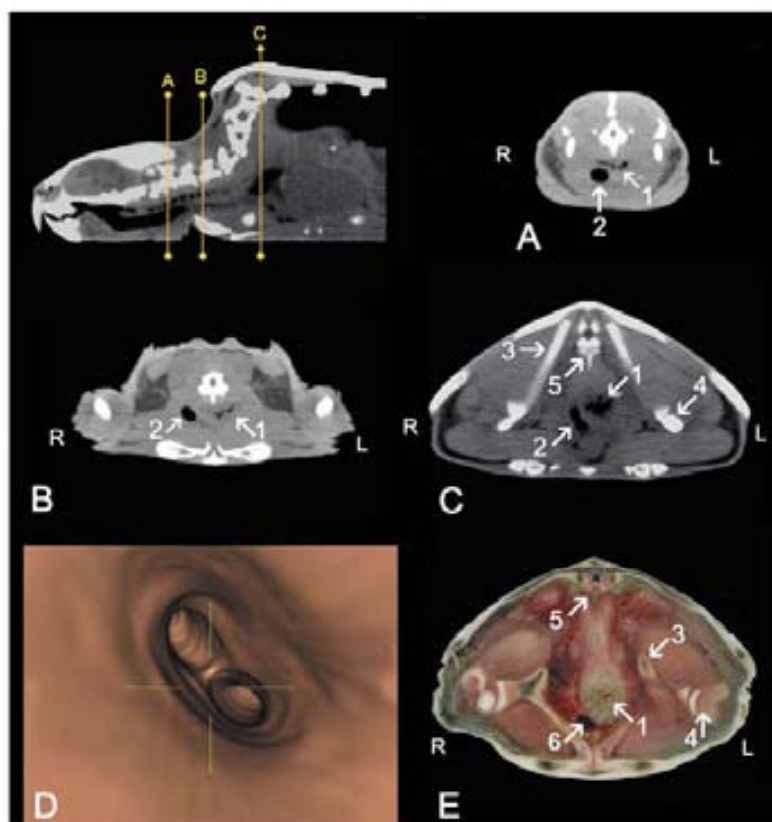


Fig. 5. (A–C) Computed tomography images, transverse plane – soft-tissue window, (D) virtual bronchoscopy image and (E) corresponding gross anatomical section of a juvenile loggerhead sea turtle. 1, oesophagus; 2, trachea; 3, scapula; 4, humerus head; 5, 1st dorsal vertebra; 6, carina. D, internal view of the tracheal bifurcation (carina).

Please cite this article in press as: Valente, A.L.S. et al., Computed tomography of the vertebral column and coelomic ..., Vet. J. (2006), doi:10.1016/j.tvjl.2006.08.018

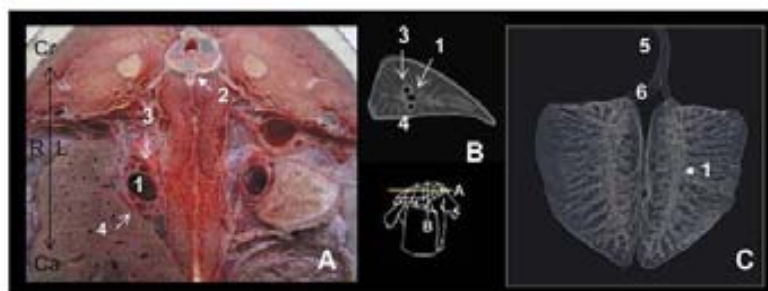


Fig. 6. (A) Dorsal gross anatomical section, (B) multiplanar CT (transverse plane – soft-tissue window) and (C) 3D CT reconstructions of the respiratory tract of the loggerhead sea turtle. 1, bronchus; 2, 6th cervical vertebra; 3, pulmonary artery; 4, pulmonary vein; 5, trachea; 6, extrapulmonary bronchus.

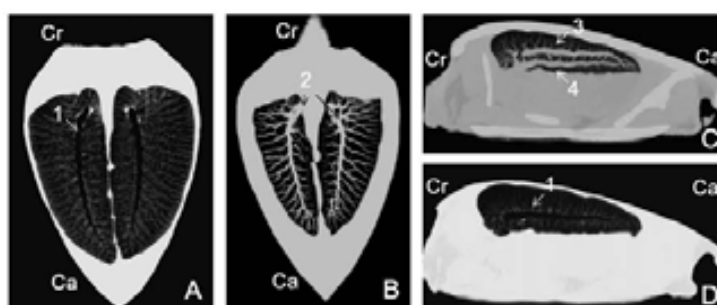


Fig. 7. Multiplanar CT reconstructions, (A, B – dorsal plane, C, D – sagittal plane; both with CT lung window) of the lungs of a juvenile loggerhead sea turtle. 1, central bronchus; 2, pulmonary vasculature; 3, pulmonary artery; 4, pulmonary vein.

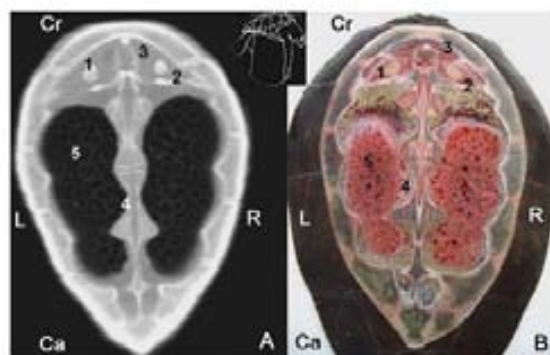


Fig. 8. (A) Multiplanar reconstruction (dorsal plane – soft-tissue window) and (B) corresponding gross anatomical section of a small juvenile loggerhead sea turtle. 1, scapula; 2, 1st pair of ribs; 3, 8th cervical vertebra; 4, 3rd dorsal vertebra; 5, pulmonary parenchyma.

trum are concave, and instead of a typical intervertebral disc with *nucleus pulposus* as occurs in mammals (*acoelous*), a cartilage plug is present in the intervertebral spaces. This kind of centrum is a feature of early reptiles' vertebrae that did not apparently move very much relative to one another (Williston, 1914), as is the case with the turtles' dorsal vertebrae. Information concerning the vertebral column of the loggerhead sea turtle is scarce. Wyncken (2001) described

the general vertebral gross anatomy of the sea turtle. However, detailed information focusing on vertebral morphology and its arrangement was not provided.

Knowledge of the intervertebral foramina position and the morphology of each vertebra obtained with MDCT could also potentially improve the evaluation of the spinal cord and nerve roots in magnetic resonance images of turtles with carapace injuries associated with neurological signs. These may result from propeller or hull impact, shark-bite wounds, and the action of fishermen who may deliberately cause head trauma to turtles presumed to have reduced catches or damaged equipment (Panagopoulos et al., 2001; McArthur, 2004; Parga et al., 2005).

Although CT is not the most suitable diagnostic technique to evaluate soft tissues we have obtained good images of the heart, stomach, liver, gallbladder, kidneys and some parts of the intestine. Due to the flattened shape of the turtle's body in the dorsoventral direction and the unusual dorsal position of the lungs, CT images of the turtles' coelomic cavity differ from those observed in domestic animals such as the dog and cat (De Rycke et al., 2005; Samii et al., 1998). In transverse CT images of the thoracic cavity of dogs and cats using the lung setting it is possible to identify the heart, large vessels and anatomical structures in the mediastinal region because of the contrast formed by the lungs, which almost totally fill the thoracic cavity. The position of the heart of the loggerhead sea

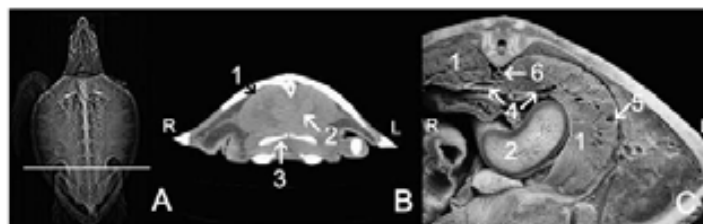


Fig. 9. Transverse CT image (soft-tissue window) of the renal region and corresponding anatomical section of a juvenile loggerhead sea turtle. A, section location; B: 1, kidneys; 2, intestinal loop; 3, pubic bones. C: 4, renal veins; 5, branch of the external iliac vein. 6, aorta artery.

turtle, with the atria limited cranially by the pectoral muscles and the ventricle limited laterally by the hepatic lobes, does not provide the air-tissue interface contrast usually observed in CT images of the mammalian thorax. On the other hand, the normal difference in density of these organs made it possible to distinguish them. In juvenile loggerhead sea turtles a wide window between the left and right hyoplastron was observed in our study, which coincided with the cardiac area. The position of the heart was similar to that found in the tortoise and other turtles. However in these species, the hyoplastron bones and endoplastron are joined close together forming an unique bony plate covering the whole ventral surface of the coelomic cavity (McArthur et al., 2004). The bone gap in the plastron of young loggerhead sea turtles may make them more vulnerable to compressive injury when accidentally captured in trawling nets.

In this study, we have verified that MDCT is a useful tool to identify the position of the oesophagus and its relationship with the trachea and bronchia. This could help clinicians to evaluate the extent of damage produced by an accidentally swallowed fishhook caught in the digestive tract and determine the best way to access it in a surgical procedure. Since perforating oesophageal lesions could secondarily affect the larynx (Orós et al., 2005), and therefore the upper airways, virtual bronchoscopy could be used to evaluate airway integrity.

One of the most important clinical contributions of CT examination is in relation to the pulmonary system. Cranio-caudal and lateral radiographic views are normally used for detecting pulmonary diseases in chelonians (Hernandez-Divers and Hernandez-Divers, 2001). However, when associated with fracture of the carapace, local inflammatory response and bone fragment superimposition usually impede an accurate evaluation of the pulmonary parenchyma. Multi-detector computed tomography provides accurate information on the lungs and airways because the slow respiratory rate of chelonians associated with the lung-air contrast permits high quality visualization of the lungs and the airways. The general morphology of the respiratory tract of loggerhead sea turtles described in our work is consistent with that of a previous histological work performed in hatchlings of this species (Fleetwood and Munnell, 1996). The position of the carina found in

our study appear to be slightly more caudal than in land tortoises, in which the trachea bifurcates after coursing a relatively short distance down the neck (Murray, 2006). The difference in the position of carina in this case seems to be related with the morpho-functional characteristic of the neck observed in different groups of the Testudines. In tortoises and most turtles (Cryptodira) the neck vertebrae flex vertically, allowing the head to be drawn straight back within the shell. In these species the most cranial position of the carina allows breathing even when the head and neck are withdrawn. As in sea turtles the ability to retract the head has been lost (Pecor, 2003), the relatively caudal position of the bronchial bifurcation does not cause any breathing impediment.

In chelonians in particular, the anatomy of the lower respiratory tract is of clinical importance. Inflammatory exudates particularly those associated with infectious diseases tend to accumulate in the dependent portion of the lung. This location precludes timely elimination through the bronchi and trachea as one would expect in mammalian patients (Murray, 1996). Pneumonia in the red-eared slider (*Trachemys scripta*) has been detected in slightly paramedian sagittal CT scans in which the normal reticular lung pattern is found to be missing (Wilkinson et al., 2004).

The kidneys of sea turtles are located retroperitoneally between the peritoneum and the shell and differ in the morphology and angio-architecture from those found in mammals (Wyneken, 2001). They are metanephric and lack a distinct cortex, medulla and renal pelvis. The kidneys were seen as a homogeneous parenchyma in CT images contrasting only with the peripheral fat present between them and the carapace.

The general anatomy of loggerhead sea turtles is comparable to that found in other chelonian species but with differences in the relative size of some organs. For instance, the lungs of tortoises seem to have much more volume than those of the loggerhead sea turtle. In transverse section at level of the heart base, in a tortoise the lungs occupy about two-thirds of the height of the coelomic cavity (Wilkinson et al., 2004), whereas in loggerhead sea turtles they are only in the dorsal third of this cavity. In the former, this organ has a pyramidal shape tapering in its caudal end, and in the latter the lungs are more flattened. In addition, the pectoral

musculature in loggerhead sea turtles observed in this study was more developed than that of tortoises (Wilkinson et al., 2004).

The use of MDCT allowed a fast examination, multiplanar reconstructions and an excellent 3D volume rendering which provided assessment of the skeleton and lung morphology in great detail. Comparison with the anatomical sections was indispensable in our study to recognize the parenchymatous organs in the CT images, although it was difficult to distinguish abdominal soft-tissue structures such as intestine portions, pancreas and reproductive organs because of their small size and/or a lack of contrast between them and the surrounding tissues.

5. Conclusions

Computed tomography solves problems of superimposed skeletal structures seen in plain radiographs and can be used to evaluate fractures, luxations, bone demineralization, neoplasia and visceral calcifications.

The slow respiratory rate of reptiles associated with the lung-air contrast allowed the lungs to be visualized in detail, suggesting that this may be a technique potentially suitable for diagnosing a great variety of pulmonary pathologies. The morphology of the lung of juvenile loggerhead sea turtles seen using MDCT is consistent with the morphology reported in a previous histological study performed in hatchlings of the same species. Compared to other diagnostic imaging modalities, MDCT provides excellent information about the respiratory system and skeleton in a short examination time, thereby minimizing the risks of anaesthesia. The location of the coelomic structures with respect to the carapace and the vertebrae that is provided in this work will facilitate the examination and interpretation of other ancillary diagnostic techniques such as ultrasound and X-rays, improving safety of access in biopsies and surgical procedures as a result.

Acknowledgements

The authors thank Professor Dr. Francisco Reina and technician Isabel Delgado Calvarro, Facultad de Medicina, UAB, for their help with the anatomical sections, and the radio-diagnostic technician Montse March for technical support with the MDCT.

References

- Abou-Madi, N., Scrivani, P., Kollias, G.V., Hernandez-Divers, S.M., 2004. Diagnosis of skeletal injuries in chelonians using computed tomography. *Journal of Zoo and Wildlife Medicine* 35, 226–231.
- Arencibia, A., Rivero, M.A., Cusal, A.B., González-Romano, N., Orós, J., 2005. CT and Cross-sectional Anatomy of the Normal Head of the Loggerhead Sea Turtle (*Caretta caretta*). *Anatomia, Histologia, Embryologia* 34, 3.
- ASIH/HL/SSAR., 2001. Guidelines for use of live amphibians and reptiles in field research. American Society of Ichthyologists and Herpetologists (ASIH), The Herpetologists' League (HL) and Society for the Study of Amphibians and Reptiles (SSAR), pp. 1–20. Available from: <http://www.asih.org/pubs/herpcoll.html>. Accessed 4 July 2006.
- De Rycke, L., Gielen, I.M., Simoons, P.J., Bree, H.V., 2005. Computed tomography and cross-sectional anatomy of the thorax in clinically normal dogs. *American Journal of Veterinary Research* 66, 512–524.
- Fleetwood, J.N., Munnell, J.F., 1996. Morphology of the airways and lung parenchyma in hatchlings of the loggerhead sea turtle, *Caretta caretta*. *Journal of Morphology* 227, 289–304.
- Gaffney, E.S., 1990. The comparative osteology of the Triassic turtle *Proganochelys*. *Bulletin of the American Museum of Natural History* 194, 1–263.
- Garland, M.R., Lawler, L.P., Whitaker, B.R., Walker, I.D.F., Corl, F.M., Fishman, E.K., 2002. Modern CT applications in veterinary medicine. *Radiographics* 22, 55–62.
- Gaudron, C., Lignereux, Y., Ducos de Lahitte, J., 2001. Imagerie médicale appliquée à l'anatomie clinique des chéloniens en consultation. In: *Proceedings of the International Congress on Testudo Genus*, pp. 161–179.
- Gumpenberger, M., Henninger, W., 2001. The use of computed tomography in avian and reptile medicine. *Seminars in Avian and Exotic Pet Medicine* 10, 174–180.
- Hernandez-Divers, S., Hernandez-Divers, S., 2001. Diagnostic imaging of reptiles. In *Practice* July/August, 370–391.
- McArthur, S., 2004. Problem-solving approach to conditions of marine turtles. In: McArthur, S., Wilkinson, R., Jean, M. (Eds.), *Medicine and Surgery of Tortoises and Turtles*. Blackwell Publishing Ltd., Victoria, Australia, pp. 301–307.
- McArthur, S., Meyer, J., Innis, C., 2004. Anatomy and physiology. In: McArthur, S., Wilkinson, R., Jean, M. (Eds.), *Medicine and Surgery of Tortoises and Turtles*. Blackwell Publishing Ltd., Victoria, Australia, pp. 35–72.
- Murray, M.J., 1996. Pneumonia and normal respiratory function. In: Mader, Douglas R. (Ed.), *Reptile Medicine and Surgery*. WB Saunders Co., Philadelphia, pp. 396–405.
- Murray, M.J., 2006. Cardiopulmonary anatomy and physiology. In: Mader, Douglas R. (Ed.), *Reptile Medicine and Surgery*. Elsevier Inc., Philadelphia, pp. 124–134.
- Orós, J., Torrent, A., Calabuig, P., Déniz, S., 2005. Diseases and causes of mortality among sea turtles stranded in the Canary Islands, Spain (1998–2001). *Diseases of Aquatic Organisms* 63, 13–24.
- Panagopoulos, D., Sofouli, E., Teneketzis, K., Margaritoulis, D., 2001. Stranding data as an indicator of fisheries induced mortality of sea turtles in Greece. In: *Proceedings of the 1st Mediterranean Conference on Marine Turtles*, Rome, Italy.
- Parga, M., Valente, A.L., Zamora, M.A., Lavin, S., Alegre, F., Cuenca, R., Marco, I., 2005. Carapace trauma associated with hind limb paralysis in a loggerhead sea turtle. In: *Proceedings of the Spring Meeting of the British Veterinary Zoological Society* 200, p. 41.
- Pecor, K., 2003. "Testudines" (On-line). Animal Diversity Web. Available from: <http://animaldiversity.ummz.umich.edu/site/accounts/information/Testudines.html>. Accessed 5 July 2006.
- Pont, S.G., Alegre, F.N., 2000. Work of the foundation for the conservation and recovery of marine life. *Marine Turtle Newsletter* 87, 5–7.
- Raïti, P., 1998. The use of computerized tomography and magnetic resonance imaging in chelonian medicine. In: *Proceedings of the Association of Reptilian and Amphibian Veterinarians*, pp. 51–53.
- Raïti, P., Haramati, N., 1997. Magnetic resonance imaging and computerized tomography of a gravid leopard tortoise (*Geochelone pardalis*) with metabolic bone disease. *Journal of Zoo and Wildlife Medicine* 28, 189–197.
- Samii, V.F., Biller, D.S., Koblak, P.D., 1998. Normal cross-sectional anatomy of the feline thorax and abdomen: comparison of computed tomography and cadaver anatomy. *Veterinary Radiology and Ultrasound* 39, 504–511.

- Wilkinson, R., Hernandez-Divers, S., Lafortune, M., Calvert, I., Gumpenberger, M., McArthur, S., 2004. Diagnostic imaging. In: McArthur, S., Wilkinson, R., Jean, M. (Eds.), *Medicine and Surgery of Tortoises and Turtles*. Blackwell Publishing Ltd., Victoria, Australia, pp. 187–238.
- Williston, S.W., 1914. *Water reptiles of the past and present*. Arment Biological Press, Landisville, PA, p. 156.
- Wyncken, J., Wilke, W.D., Steinberg, F., 2000. Looking at turtles in three dimensions. In: *Proceedings of the 20th Annual Sea Turtle Symposium, Orlando, Florida*, pp. 106–107.
- Wyncken, J., 2001. *The Anatomy of Sea Turtles*. U.S. Department of Commerce NOAA Technical Memorandum NMFS-SEFSC 470, pp. 1–172.

